Optics Letters

Attosecond photoelectron streaking with enhanced energy resolution for small-bandgap materials

Alexander Guggenmos,[1,2,*,†] Ayman Akil,[1,2,4,†] Marcus Ossiander,[2,3] Martin Schäffer,[2,3] Abdallah Mohammed Azzeer,[4] Gerhard Boehm,[5] Markus-Christian Amann,[5] Reinhard Kienberger,[2,3] Martin Schultze,[1,2] and Ulf Kleineberg[1,2]

[1]Fakultät für Physik, Ludwig-Maximilians-Universität München, Am Coulombwall 1, D-85748 Garching, Germany
[2]Max-Planck-Institut für Quantenoptik, Hans-Kopfermann-Strasse 1, D-85748 Garching, Germany
[3]Physik-Department, Technische Universität München, James-Frank-Strasse 1, D-85748 Garching, Germany
[4]Physics and Astronomy Department, King Saud University, Riyadh 11451, Saudi Arabia
[5]Walter Schottky Institut, Technische Universität München, Am Coulombwall 4, D-85748 Garching, Germany
*Corresponding author: alexander.guggenmos@physik.lmu.de

Received 30 June 2016; accepted 12 July 2016; posted 13 July 2016 (Doc. ID 269551); published 3 August 2016

Attosecond photoelectron streaking spectroscopy allows time-resolved electron dynamics with a temporal resolution approaching the atomic unit of time. Studies have been performed in numerous systems, including atoms, molecules, and surfaces, and the quest for ever higher temporal resolution called for ever wider spectral extent of the attosecond pulses. For typical experiments relying on attosecond pulses with a duration of 200 as, the time-bandwidth limitation for a Gaussian pulse implies a minimal spectral bandwidth larger than 9 eV translating to a corresponding spread of the detected photoelectron kinetic energies. Here, by utilizing a specially tailored narrowband reflective XUV multilayer mirror, we explore experimentally the minimal spectral width compatible with attosecond time-resolved photoelectron spectroscopy while obtaining the highest possible spectral resolution. The validity of the concept is proven by recording attosecond electron streaking traces from the direct semiconductor gallium arsenide (GaAs), with a nominal bandgap of 1.42 eV at room temperature, proving the potential of the approach for tracking charge dynamics also in these technologically highly relevant materials that previously have been inaccessible to attosecond science.

OCIS codes: (320.0320) Ultrafast optics; (120.3940) Metrology; (230.4170) Multilayers; (230.4040) Mirrors.

http://dx.doi.org/10.1364/OL.41.003714

Attosecond electron streaking experiments of electron wave packet dynamics in gases [1] or metals [2] aim mainly for a high temporal resolution, while an additional high spectral resolution is usually not required [3]. This changes dramatically if semiconductors are investigated. Based on their electron band structure, they demand both high temporal and high spectral resolution for the investigation of characteristic band dynamics as was recently demonstrated in silicon [4] based on transient absorption spectroscopy [5]. The spectral resolution of experiments providing attosecond temporal resolution is limited by the minimal required spectral bandwidth of sub-femtosecond pulses which resulted in typical previous experiments in a spectral bandwidth in the range of 5–30 eV [6]. This precluded materials with narrower spectral signatures from being studied.

Here we explore the minimal spectral extent required to achieve both an attosecond temporal and a high spectral resolution in an electron streaking experiment with single attosecond pump pulses and few-cycle near-infrared (NIR) probe pulses [7]. Streaking of (multi-)fs electron wave packets has been also realized by THz streaking fields [8] with a high spectral resolution, but on the expense of the loss of attosecond temporal resolution. An alternative approach may be based on attosecond pulse trains with intrinsically narrowband and attosecond temporal resolution being applied in a RABBITT [9,10] measurement, but the nonambiguous correlation of sub-fs electron dynamics in matter is difficult.

The dominating generation process for isolated attosecond pulses in the extreme ultraviolet (XUV) is high-harmonic generation (HHG) in gases [11,12], driven by intense phase-stabilized few-cycle laser pulses [7], and consecutive spectral filtering of the cutoff region by means of a thin metal filter [13] and a monochromatizing multilayer mirror [14]. Other methods for generating isolated attosecond pulses are based on polarization gating [15], intensity gating [16], or the lighthouse effect [17]. In attosecond electron streaking experiments, these attosecond XUV pulses are commonly focused by a multilayer mirror onto the target to be investigated to photoionize the target atoms. The freed photoelectrons are then momentum streaked by the co-propagating NIR vector potential [18]. There exists a theoretical upper limit of the attosecond pulse duration, accompanied by the spectral resolution of the exciting extreme ultraviolet pulse, where clean electron streaking is still possible [19]: $\Delta\tau = T_{\mathrm{NIR}}/2$, with the attosecond pulse duration $\Delta\tau$ and the electric field period T_{NIR} of the NIR pulse. The streaking characteristic vanishes for longer attosecond

pulses, translating into longer electron wave packets and changes to a sideband [20] pronounced spectrum [19].

As the spectral resolution and attosecond pulse duration is mainly determined by the multilayer mirror, we have set a full width at half-maximum (FWHM) bandwidth of $\Delta E = 1.8$ eV for the mirror's reflectivity profile as spectral resolution limit for our experimental investigation. Periodic molybdenum/boron carbide (Mo/B_4C) layers were chosen for a central energy at 112 eV (5° normal incidence), filtering isolated attosecond pulses from the HHG cutoff region close to a Gaussian pulse Fourier limit of 1000 as, and for a spectral streaking resolution of about 1.8 eV. This allows for single attosecond pump pulses covering various core levels (Ga 3d at 18.7 eV, Ga 3p ~100 eV, As 3d at 41.7 eV) combined with a high spectral resolution for differing spectrally, e.g., the valence and conduction band of GaAs. The spectral characterization of the realized mirror was carried out on a witness sample at the Physikalisch-Technische Bundesanstalt (PTB) beamline at BESSY II in Berlin and is shown in Fig. 1.

The spectral measurement indicates a slight shift of the center energy by 0.6 eV due to deposition effects [21], but an excellent agreement with the target bandwidth of $\Delta E = 1.8$ eV. Other multilayer material systems may exhibit a higher peak reflectivity in this energy range, but either contain toxic material (Mo/Be [22]), are not stable, and show long-term degradation (Mo/Sr [23]) or suffer from strong spectral modulations around the Bragg peak by Kiessig fringes (Mo/Y [24]) and, therefore, introduce additional group delay dispersion (GDD) which broadens the pulse in the time domain [25]. Therefore, we have chosen Mo/B_4C as a material system fulfilling the experimental demands on high and temporally stable peak reflectivity, small spectral bandwidth, and a linear spectral phase (advantage of periodic compared to aperiodic).

The material system Mo/B_4C allows, in principle, a more precise determination of the spectral resolution limit for attosecond electron streaking experiments by accurately tuning the multilayer design parameters. The spectral bandwidth of a multilayer mirror at a certain central energy can be influenced by the number of periods N (dependent on the contributing period number) and the layer thickness ratio γ (bottom layer thickness versus period thickness d). For example, a spectral bandwidth of ~500 meV has been realized in the case of Mo/Si multilayer mirrors [26] for filtering a single high-harmonic peak utilizing 300 bilayers and a gamma (d_{Mo}/d) of $\gamma = 0.04$ at a central photon energy of 97 eV. The simulated peak reflectivity and the corresponding spectral bandwidth are dependent on both the number of periods N and the ratio γ and are for the Mo/B_4C system depicted in Fig. 2(c). Our previous investigations have revealed a high film stress within the Mo/B_4C stack for a strong detuning ratio γ and a high period number N (resulting in a high overall stack height). The strain-induced delamination process of the coating after the deposition is independent on capping or adhesion layers, as well as on the substrate material (fused silica substrate or silicon wafer), as shown in Fig. 2(b). As we have set an experimental spectral bandwidth limit of $\Delta E = 1.8$ eV for electron streaking, we defined a maximum stack height of 400 nm to prevent a high stress within the coating. This demand resulted in a final gamma ratio of $\gamma = 0.35$ and a period number of $N = 70$ facilitating the realization of the coating without delamination, as shown in Fig. 2(a).

Optimizing the deposition process [27] may allow larger period numbers and a lower gamma ratio, resulting in a lower spectral bandwidth and a more accurate experimental determination of the spectral resolution limit.

To extract both the temporal and spectral resolution of the attosecond pulses on reflection from the previously calibrated molybdenum/boron carbide multilayer mirror, we have used the well-established XUV pump/NIR probe electron streaking technique thoroughly explained in [18]. On one hand, this experiment confirms the previously achieved results, since the spectral and temporal resolution is mainly determined by the mirror; on the other hand, it proves the realization of electron streaking with enhanced energy resolution for future investigation of small-bandgap materials.

Here, attosecond pulses are generated by HHG in a neon (Ne) gas jet using carrier-envelope phase-stabilized sub-4 fs NIR pulses (160 mbar, $\Delta\tau < 4$ fs, 0.5 mJ, $f = 55$ cm). This results in an HH cutoff spectrum ranging from 100 to

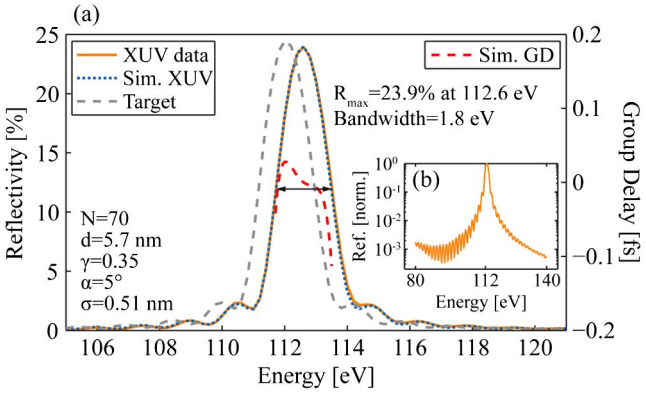

Fig. 1. (a) Measured spectral reflectivity profile (solid orange) of the realized Mo/B_4C multilayer mirror, its fit (dotted blue), the target profile centered at 112 eV (dashed gray), and the corresponding simulated GD (dashed red) within the bandwidth of $\Delta E = 1.8$ eV. The multilayer design parameters are listed bottom left. (b) Small inset depicts the complete spectral range of the normalized measured reflectivity profile indicating a high suppression of lower and higher frequency components (no filter transmission profile included).

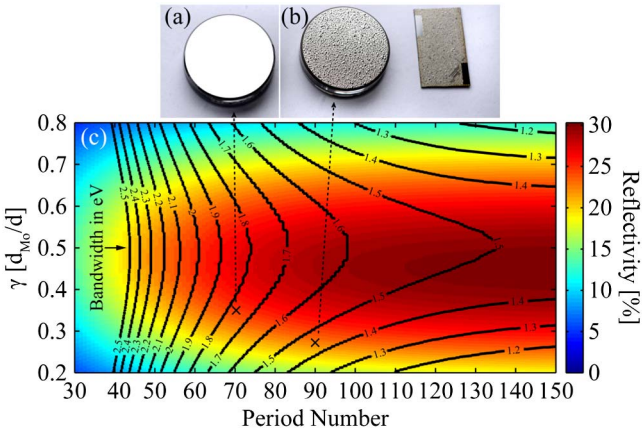

Fig. 2. (a) + (b) Mirror picture without and with delaminating multilayer coating. (c) Simulated reflectivity dependence on the gamma ratio $\gamma = d_{Mo}/d$ and the number of periods N for the Mo/B_4C material system centered at 112 eV. The corresponding spectral bandwidths in the eV unit are additionally depicted as black contour lines.

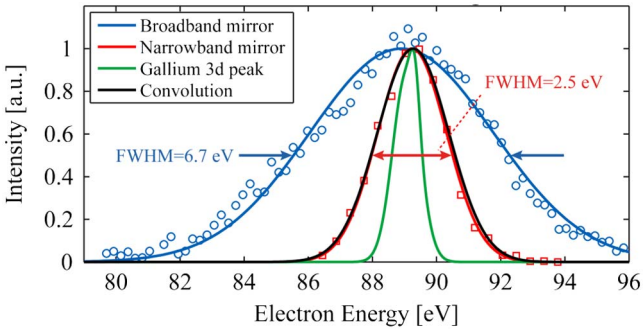

Fig. 3. Unstreaked photoelectron spectra of the gallium 3d peak measured with a broadband (FWHM = 5 eV) multilayer mirror (blue) and with the narrowband (FWHM = 1.8 eV) Mo/B_4C mirror (red). The circles and squares, respectively, represent the data points, whereas the solid lines depict the corresponding Gaussian fit. The convolution (black) of our TOF ~1% energy resolution, the mirror, and the gallium 3d spectrum (green) from [31] agrees with our measurement.

120 eV. The narrowband Mo/B_4C multilayer (double) mirror is used subsequently, together with a 200 nm thick zirconium filter, for spectrally filtering at $E_{\text{center}} = 112$ eV and focusing the attosecond pulses and the co-propagating NIR pulses onto the surface of a (100) gallium arsenide (GaAs) sample. The liberated photoelectrons from the Ga 3d core level are then momentum streaked by the temporally synchronized and phase-stabilized NIR.

Previous electron streaking measurements have shown that utilizing a broadband mirror is not adequate to spectrally resolve the bands of GaAs and have led to the development of the previously described narrowband mirror. A comparison of raw data photoelectron emission spectra (unstreaked regime) from the gallium 3d peak using a broadband, and the previously characterized narrowband XUV multilayer mirror is depicted in Fig. 3.

The streaking spectrogram in Fig. 4(a) is formed through measuring the delay dependent photoelectron energy and intensity. The measurement shows a well-pronounced streaking trace, although the spectral bandwidth and the linear phase of the mirror suggest an attosecond pulse duration of approximately half that of the probing NIR period. FROG/CRAB [28,29] analysis is performed to retrieve the spectrogram of Fig. 4(b), and to extract the intensity and group delay of the electron wave packet in Fig. 4(c), as well as the vector potential of the streaking NIR pulse. The measured and retrieved photoelectron streaking spectrograms in Figs. 4(a) and 4(b) are shifted by the binding energy of the Ga 3d core level ($E_b = 18.7$ eV) and the work function of GaAs ($E_{\text{WF}} = 4.69$ eV) [30] away from the central energy of the mirror. The spectral characteristic of the retrieved electron wave packet in Fig. 4(c) shows a spectral bandwidth (FWHM) of 2.8 eV which is 1 eV larger than the measured reflectivity profile value. This is attributed to the precision of the used time of flight (TOF) electron spectrometer (1% energy resolution) and the nonresolved double structure of the gallium 3d peak [31]. A convolution of the gallium 3d peak from [31], the mirror and our TOF energy resolution are shown in Fig. 3 and agree with the fit of our unstreaked gallium 3d measurement. This bandwidth spread in the spectral domain leads to a shorter pulse duration of 780 ± 25 as in the time domain than was expected from the mirror characterization; see Fig. 4(d). The retrieved electric field of the NIR pulse in Fig. 4(e) is calculated from the retrieved NIR vector potential, which is shown as an eye-guiding white line in Fig. 4(b), and indicates an electric field period of approximately 2.1 fs. This is approximately 2.5 times the pulse duration of the

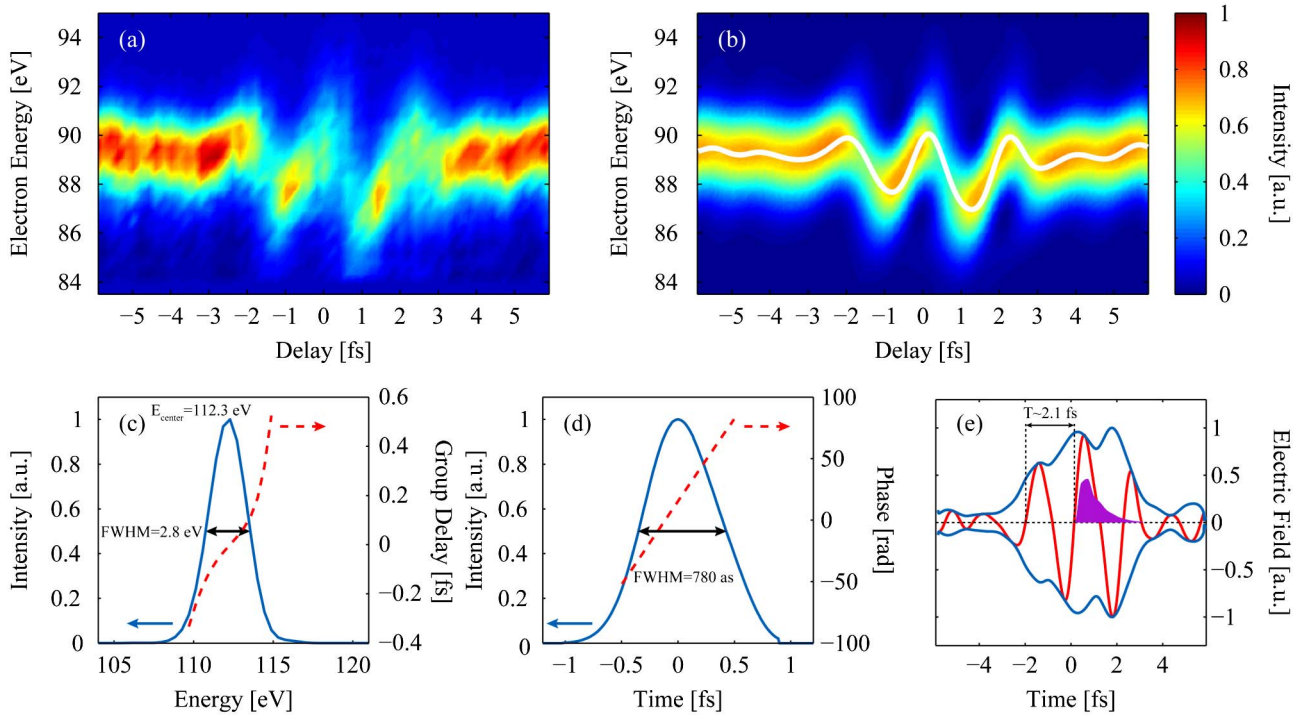

Fig. 4. (a) Measured and (b) retrieved electron streaking on GaAs. The white line in (b) depicts the retrieved vector potential A(t) of the NIR. (c) Retrieved photoelectron wave packet intensity (solid blue) and GD (dashed red) in the spectral domain. (d) Intensity and phase in the temporal domain. (e) Calculated electric field of the NIR (solid red), the envelope (solid blue), and the simulated XUV pulse (purple).

retrieved pulse. The convolution of the HHG cutoff (linear decrease and linear phase), the mirror parameters (simulated reflectivity profile and phase), and the simulated transmission property of a 200 nm thick zirconium filter (phase profile included) lead to the theoretical purple XUV pulse in Fig. 4(e). The theoretical XUV pulse shows a pulse duration of 870 as and, together with the retrieval, is close to the theoretical limit for clean attosecond streaking. The discrepancy of the group delay of Figs. 1 and 4(c) may be attributed to a small chirp of the harmonics or temporal effects in solids [32]. Besides the spectral bandwidth of the multilayer mirror, we identified the modifiable parameters to receive a clean electron streaking trace to be the NIR carrier-envelope phase (CEP), the relative focus position of both pulses, and adjusted the neon gas pressure. This influences not only the cutoff, but also the electric field period of the probing NIR by self-phase modulation.

So far, we have classified typical attosecond experiments in two different sections: extremely short isolated pulses [12,33] with vanishing energy resolution or setting a time and energy resolution trade-off utilizing hundreds of attoseconds with a spectral bandwidth below 10 eV. We have opened the door for the third section: utilizing long attosecond pulses combined with a sub-2 eV energy resolution.

In summary, we have shown attosecond electron streaking on GaAs with a high spectral resolution of $\Delta E = 1.8$ eV at $E_\gamma = 112$ eV, close to the limit that the theory predicts [19]. This experiment paves the way for time- and spectrally-resolved attosecond experiments on GaAs and may even open the door for time-resolved XMCD (x-ray magnetic circular dichroism) measurements [34], where a high spectral resolution is required to resolve spin-orbit coupled states in the future.

Funding. Deutsche Forschungsgemeinschaft (DFG) (EXC158); King Saud University (KSU) (IRG14-07A); Munich-Centre for Advanced Photonics (MAP).

Acknowledgment. The authors are grateful for the scientific support and valuable discussions with Ferenc Krausz (MPQ, LMU) and the King-Saud University for their support within the MPQ-KSU-LMU collaboration. R. K. acknowledges an ERC Starting Grant. The authors thank Thorsten Naeser for the mirror pictures.

†These authors contributed equally to this work.

REFERENCES

1. M. Schultze, M. Fieß, N. Karpowicz, J. Gagnon, M. Korbman, M. Hofstetter, S. Neppl, A. L. Cavalieri, Y. Komninos, T. Mercouris, C. A. Nicolaides, R. Pazourek, S. Nagele, J. Feist, J. Burgdörfer, A. M. Azzeer, R. Ernstorfer, R. Kienberger, U. Kleineberg, E. Goulielmakis, F. Krausz, and V. S. Yakovlev, Science **328**, 1658 (2010).
2. S. Neppl, R. Ernstorfer, A. L. Cavalieri, C. Lemell, G. Wachter, E. Magerl, E. M. Bothschafter, M. Jobst, M. Hofstetter, U. Kleineberg, J. V. Barth, D. Menzel, J. Burgdörfer, P. Feulner, F. Krausz, and R. Kienberger, Nature **517**, 342 (2015).
3. R. Pazourek, S. Nagele, and J. Burgdörfer, Faraday Discuss. **163**, 353 (2013).
4. M. Schultze, K. Ramasesha, C. D. Pemmaraju, S. A. Sato, D. Whitmore, A. Gandman, J. S. Prell, L. J. Borja, D. Prendergast, K. Yabana, D. M. Neumark, and S. R. Leone, Science **346**, 1348 (2014).
5. X. Wang, M. Chini, Y. Cheng, Y. Wu, X.-M. Tong, and Z. Chang, Phys. Rev. A **87**, 063413 (2013).
6. M. Chini, K. Zhao, and Z. Chang, Nat. Photonics **8**, 178 (2014).
7. A. Baltuška, T. Udem, M. Uiberacker, M. Hentschel, E. Goulielmakis, C. Gohle, R. Holzwarth, V. S. Yakovlev, A. Scrinzi, T. W. Hänsch, and F. Krausz, Nature **421**, 611 (2003).
8. B. Schütte, S. Bauch, U. Frühling, M. Wieland, M. Gensch, E. Plönjes, T. Gaumnitz, A. Azima, M. Bonitz, and M. Drescher, Phys. Rev. Lett. **108**, 253003 (2012).
9. H. G. Muller, Appl. Phys. B **74**, s17 (2002).
10. S. B. Schoun, R. Chirla, J. Wheeler, C. Roedig, P. Agostini, and L. F. DiMauro, Phys. Rev. Lett. **112**, 153001 (2014).
11. M. Hentschel, R. Kienberger, C. Spielmann, G. A. Reider, N. Milosevic, T. Brabec, P. Corkum, U. Heinzmann, M. Drescher, and F. Krausz, Nature **414**, 509 (2001).
12. K. Zhao, Q. Zhang, M. Chini, Y. Wu, X. Wang, and Z. Chang, Opt. Lett. **37**, 3891 (2012).
13. E. Magerl, S. Neppl, A. L. Cavalieri, E. M. Bothschafter, M. Stanislawski, T. Uphues, M. Hofstetter, U. Kleineberg, J. V. Barth, D. Menzel, F. Krausz, R. Ernstorfer, R. Kienberger, and P. Feulner, Rev. Sci. Instrum. **82**, 063104 (2011).
14. M. Hofstetter, A. Aquila, M. Schultze, A. Guggenmos, S. Yang, E. Gullikson, M. Huth, B. Nickel, J. Gagnon, V. S. Yakovlev, E. Goulielmakis, F. Krausz, and U. Kleineberg, New J. Phys. **13**, 063038 (2011).
15. I. J. Sola, E. Mével, L. Elouga, E. Constant, V. Strelkov, L. Poletto, P. Villoresi, E. Benedetti, J.-P. Caumes, S. Stagira, C. Vozzi, G. Sansone, and M. Nisoli, Nat. Phys. **2**, 319 (2006).
16. T. Pfeifer, M. J. Abel, P. M. Nagel, W. Boutu, M. J. Bell, Y. Liu, D. M. Neumark, and S. R. Leone, Opt. Lett. **34**, 1819 (2009).
17. T. J. Hammond, G. G. Brown, K. T. Kim, D. M. Villeneuve, and P. B. Corkum, Nat. Photonics **10**, 171 (2016).
18. R. Kienberger, E. Goulielmakis, M. Uiberacker, A. Baltuska, V. Yakovlev, F. Bammer, A. Scrinzi, T. Westerwalbesloh, U. Kleineberg, U. Heinzmann, M. Drescher, and F. Krausz, Nature **427**, 817 (2004).
19. M. Drescher, M. Hentschel, R. Kienberger, M. Uiberacker, V. Yakovlev, A. Scrinzi, T. Westerwalbesloh, U. Kleineberg, U. Heinzmann, and F. Krausz, Nature **419**, 803 (2002).
20. S. Haessler, B. Fabre, J. Higuet, J. Caillat, T. Ruchon, P. Breger, B. Carré, E. Constant, A. Maquet, E. Mével, P. Salières, R. Taïeb, and Y. Mairesse, Phys. Rev. A **80**, 011404 (2009).
21. A. Guggenmos, R. Rauhut, M. Hofstetter, S. Hertrich, B. Nickel, J. Schmidt, E. M. Gullikson, M. Seibald, W. Schnick, and U. Kleineberg, Opt. Express **21**, 21728 (2013).
22. S. Bajt, J. Vac. Sci. Technol. A **18**, 557 (2000).
23. B. Sae-Lao and C. Montcalm, Opt. Lett. **26**, 468 (2001).
24. C. Montcalm, B. T. Sullivan, S. Duguay, M. Ranger, W. Steffens, H. Pépin, and M. Chaker, Opt. Lett. **20**, 1450 (1995).
25. A. Guggenmos, M. Jobst, M. Ossiander, S. Radünz, J. Riemensberger, M. Schäffer, A. Akil, C. Jakubeit, P. Böhm, S. Noever, B. Nickel, R. Kienberger, and U. Kleineberg, Opt. Lett. **40**, 2846 (2015).
26. E. M. Gullikson, C. N. Anderson, S.-S. Kim, D. Lee, R. Miyakawa, F. Salmassi, and P. P. Naulleau, Appl. Opt. **54**, 4280 (2015).
27. A. Guggenmos, S. Radünz, R. Rauhut, M. Hofstetter, S. Venkatesan, A. Wochnik, E. M. Gullikson, S. Fischer, B. Nickel, C. Scheu, and U. Kleineberg, Opt. Express **22**, 26526 (2014).
28. R. Trebino, K. W. DeLong, D. N. Fittinghoff, J. N. Sweetser, M. A. Krumbügel, B. A. Richman, and D. J. Kane, Rev. Sci. Instrum. **68**, 3277 (1997).
29. J. Gagnon, E. Goulielmakis, and V. S. Yakovlev, Appl. Phys. B **92**, 25 (2008).
30. D. Haneman, J. Phys. Chem. Solids **11**, 205 (1959).
31. P. Moriarty, B. Murphy, L. Roberts, A. A. Cafolla, G. Hughes, L. Koenders, and P. Bailey, Phys. Rev. B **50**, 14237 (1994).
32. W. A. Okell, T. Witting, D. Fabris, C. A. Arrell, J. Hengster, S. Ibrahimkutty, A. Seiler, M. Barthelmess, S. Stankov, D. Y. Lei, Y. Sonnefraud, M. Rahmani, T. Uphues, S. A. Maier, J. P. Marangos, and J. W. G. Tisch, Optica **2**, 383 (2015).
33. E. Goulielmakis, M. Schultze, M. Hofstetter, V. S. Yakovlev, J. Gagnon, M. Uiberacker, A. L. Aquila, E. M. Gullikson, D. T. Attwood, R. Kienberger, F. Krausz, and U. Kleineberg, Science **320**, 1614 (2008).
34. C. Boeglin, E. Beaurepaire, V. Halté, V. López-Flores, C. Stamm, N. Pontius, H. A. Dürr, and J.-Y. Bigot, Nature **465**, 458 (2010).